MR imaging parameters are indicative of malignant transformation for low grade gliomas

Llewellyn Jalbert[1], Adam Elkhaled[2], Joanna Phillips[3], Rupa Parvataneni[2], Soonmee Cha[2], Susan Chang[4], and Sarah Nelson[2,5]

[1]Bioengineering and Therapeutic Sciences, University of California, San Francisco, San Francisco, CA, United States, [2]Radiology and Biomedical Imaging, University of California, San Francisco, [3]Pathology, University of California, San Francisco, [4]Neurosurgery, University of California, San Francisco, [5]Bioengineering and Therapeutic Sciences, University of California, San Francisco

Introduction: Gliomas are heterogeneous, infiltrating tumors of the central nervous system that include astrocytomas, oligodendrogliomas, and mixed oligoastrocytomas. The prognosis for these patients can vary significantly depending on the grade of malignancy and histological characteristics, as defined by the World Health Organization (WHO) (*1*). Although patients with low grade glioma (grade II) generally live much longer than their high-grade counterparts (grades III and IV), there is substantial heterogeneity in outcome, even for individuals with the same initial diagnosis. Primary treatment is maximal safe resection, followed by radiation and/or chemotherapy at the time of progression. Many patients with tumors that are initially diagnosed as low-grade will upgrade to higher grade lesion at the time of recurrence. Previous studies have shown that *ex vivo* spectroscopy can discriminate between upgraded and non-upgraded lesions (*2*), but there are significant limitations that remain in the assessment of malignant transformation using conventional MR imaging methods. This study has applied advanced *in vivo* magnetic resonance imaging and spectroscopy techniques to characterize parameters that are associated with malignant transformation.

Methods: **Patient population** Our IRB-approved study comprised 64 patients who had previously been diagnosed with WHO grade II glioma and were presenting for surgical resection owing to suspected disease recurrence. Participants had received standard-of-care treatments that included surgical resection, radiation therapy and chemotherapy, either alone or in combination. **Preoperative MR imaging and spectroscopy** Preoperative MR examinations were conducted on a 1.5 T or 3 T EXCITE GE Signa Echospeed scanner using an 8-channel phased-array headcoil. Functional imaging included 6-directional diffusion-weighted imaging acquired in the axial plane (TR/TE=1000/108 ms, voxel size=1.7×1.7×3 mm^3, b=1000 s/mm^2) and lactate-edited 3D MR spectroscopic imaging (MRSI) using point-resolved spectroscopic selection (PRESS) for volume localization and very selective saturation (VSS) pulses for lipid signal suppression (excited volume=80×80×40 mm^3, overpress factors=1.5, TR/TE=1104/144 ms, FOV=16×16×16 cm^3, nominal voxel size 1×1×1 cm^3, flyback echo-planar readout gradient in the SI direction, 712 dwell points and 988 Hz sweepwidth) (*3*). Dynamic Perfusion Weighted Imaging (PWI) was acquired with a 5ml/s injection of 0.1mmol/kg body weight Gd-DTPA. 3D fast spin echo (FSE), as well as pre-and post-Gadolinium 3D spoiled gradient echo (SPGR) anatomic imaging sequences were acquired. **Post-processing of preoperative MR exam** *In vivo* data from the preoperative examination were transferred to a Sun Ultra 10 workstation (Sun Microsystems) for image alignment and for derivation of estimates of *in vivo* diffusion, spectroscopic, and perfusion parameters. Masks of regions of interest corresponding to the T2 lesion (T2L), non-enhancing T2 lesion (NEL), and contrast-enhancing region (CEL) were manually created. Maps of the apparent diffusion coefficient (ADC) and eigenvalues were generated on a pixel-by-pixel basis, according to a published algorithm (*4*). MRS imaging data were processed in order to quantify total choline (tCho) and *N*-acetylaspartate (NAA) levels, from which maps of the choline-to-*N*-acetyl-aspartate index (CNI) could be derived. CNI values were generated as described previously (*5*) and represent the changes in choline and NAA levels relative to normal voxels. Peak height (PH) and cerebral blood volume (CBV) were calculated using both non-parametric (*6*) and non-linear gamma-variate fit (*7*) to the ΔR2* hemodynamic curve from the perfusion data. The maps of PH and CBV were normalized to the median value within normal appearing white matter.

Image-guided tissue sampling 1-4 regions of suspected tumor were selected for intra-operative tissue sample collection using BrainLab surgical navigation software. Spherical ROIs with a diameter of 5mm were generated based on point logs recorded during the operation and used to evaluate *in vivo* parameters for individual tissue samples. Extensive histopathology analysis was performed on each sample by a board-certified neuropathologist at our institution. An exact Wilcoxon signed rank test was used to evaluate differences between non-upgraded (WHO grade II) and upgraded tumors (grades III and IV). For cases where there were multiple tissue samples obtained per patient, parameter values were averaged in order to perform the analysis. Statistical significance was assessed upon tests for which $p < 0.05$.

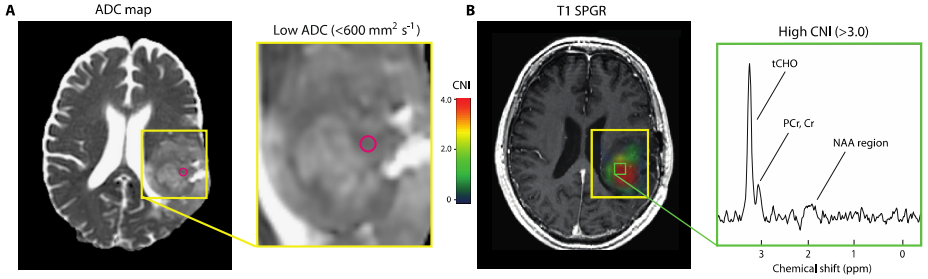

Figure 1. Representative spectroscopic (A) and diffusion imaging (B) of a WHO grade III astrocytoma displaying abnormal CNI levels associated with increased proliferation and decreased normal neuronal functioning. These MR parameters were found to reliably differentiate upgraded versus non-upgraded lesions.

Results: Histological analysis revealed 60% of the patients had lesions that converted to a higher grade at the time of resection: 26 of them remained WHO grade II, 32 converted to WHO grade III and 6 converted to WHO grade IV. For tissue samples that were characterized as upgraded versus non-upgraded there were significant differences in measures of proliferation, determined with the anti-Ki-67 antibody, increased *in vivo* measures of normalized lactate, increased normalized intensities on post-gadolinium SPGR images and increased normalized perfusion peak height. Comparisons with histological findings identified in vivo markers that corresponded to increased cellularity, proliferation, and vascular hyperplasia, and predicted malignant transformation (Figure 1). Histopathology scoring of relative tumor content (tumor score) confirmed that upgraded tumors contained increased numbers of tumor cells compared to regular cells (Figure 2). When viewed at the lesion level, parameters which distinguished upgraded tumors from non-upgraded tumors included decreased normalized ADC (nADC), decreased normalized eigenvalues corresponding to the 2nd and 3rd direction of diffusion (λ_2, λ_3); elevated CNI and normalized tCHO; as well as elevated normalized intensities in the SPGR and FSE images. Evaluation of differences in lesion volumes revealed that a number of measures of tumor burden were indicative of upgrade: increased volume of the T2L and NEL; increased volume within the T2L having decreased nADC; increased volume of elevated CNI; increased volume within the T2L having elevated PH and CBV.

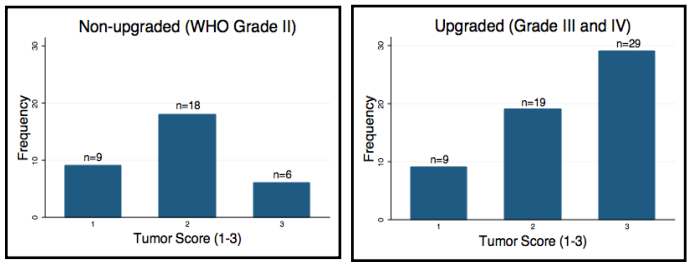

Figure 2. Histopathological scoring of tumor content confirmed that upgraded lesions contained increased tumor cellularity relative to non-upgraded lesions.

Conclusion: Direct comparisons of *in vivo* parameters with histological findings from image guided tissue samples have identified characteristics that predict whether lesions with an original diagnosis of low grade glioma have undergone malignant transformation. Analysis of metrics describing the volumes and magnitude of abnormal intensities for DWI, MRSI and PWI data have indicated that there are significant differences for lesions that have upgraded versus those that have not. This information is critical for making decisions about patient care in a timely manner.

References: [1] Grier, et al. *Oncologist* 11, 681-693 (2006) [2] Jalbert, et al. *ISMRM* 614 2010 [3] Park, et al. *Ann Biomed Eng* 39, 193-204 (2011) [4] Basset, et al. *J Magn Reson B* 111, 209-219 (1996) [5] McKnight, et al. *J Magn Reson Imaging* 13, 167-177 (2001) [6] Essock-Burns, et al. *Neuro-Oncology* 13:119–131 (2011) [7] Weiskoff et al. *ISMRM* 279 (1994) **Grant support:** *This work was supported by the NIH Brain Tumor SPORE Grant P50CA097257*